TRACTIVE PERFORMANCE OF WHEELS IN SOFT SOILS

Leslie L. Karafiath, et al

Grumman Aerospace Corporation

Prepared for:

Department of the Army

February 1973

RE-443J

TRACTIVE PERFORMANCE OF WHEELS IN SOFT SOILS

February 1973

RESEARCH DEPARTMENT

GRUMMAN AEROSPACE CORPORATION
BETHPAGE NEW YORK

Grumman Research Department Report RE-443J

TRACTIVE PERFORMANCE OF WHEELS IN SOFT SOILS†

by

Leslie L. Karafiath

and

Edward A. Nowatzki

Materials and Structural Mechanics

February 1973

†Presented at the 1972 Winter Meeting of the American Society of Agricultural Engineers in Chicago, Illinois, December 1972.

Contr-DAAE-07-72-C-0033

Approved by: Charles E. Mack, Jr.
Director of Research

1A

41

ABSTRACT

The traction developed by a wheel can be determined by appropriate integration of the soil-wheel interface stresses. In soft soils these are governed by failure conditions in the soil brought about by the wheel load. The geometry of the two failure zones (front and rear), as well as the associated stresses, constitute the solution of the differential equations of plasticity for the boundary conditions defined by the geometry of soil-wheel interface and the interface friction.

The numerical solution of the differential equations of plasticity, as well as the selection of entry and exit angles that yield matching interface stresses at the common point of the front and rear failure zones, are amenable to the application of computer techniques. A flow diagram shows the computation of failure zones and associated interface stresses that yield the load, torque, and traction for a given wheel geometry and interface friction. Slip-shear stress equations are used to relate interface friction to slip.

The solution of the practical problem of determining traction and slip for given soil conditions and applied wheel load and torque requires the iteration procedure. This is shown in another flow diagram. Inputs for the computer program schematically shown in the flow diagram are soil properties, wheel load, and torque; the end outputs are traction and slip, while entry and exit angles, interface stresses, and geometry of the failure zones can be obtained, if desired, either in the form of printed output or data files suitable for viewing on a visual display terminal.

For the computation of traction exerted by tires, a soil-tire model has been developed that allows for the deflection of

the tire and attendant restraint of the normal stresses at the interface. The front and rear failure zones are separated by a zone in which the soil is not in failure condition and the normal stress is the maximum compatible with the inflation pressure and carcass strength.

Traction values computed on the basis of soil failure conditions by the above computer program are compared with experimental results. The agreement is reasonably good when soil strength properties determined by triaxial tests are used.

NOTATIONS

c	= cohesion
DB	= drawbar pull or drag
j	= slip
j_o	= constant defining threshold slip
K	= constant in slip equation
L	= load
p_1	= limit normal stress on tire-soil interface
q_{mz}	= normal stress measured in forward field at α_m
q_{mr}	= normal stress measured in rear field at α_m
T	= torque
x,z	= geometric coordinates
α	= central angle
α',α''	= angles defining start and end of tire deflection
α_d,α_d'	= angles defining ends of flat portion of tire deflection
α_e	= entry angle

α_m = angle of separation

α_r = rear angle

γ = unit weight of soil

δ = angle of inclination of resultant stress to normal

ϵ = slope angle

λ = computed load/input load (zero subscript indicates initial value)

φ = friction angle

ψ = c cot ϕ

θ = angle enclosed by major principal stress and x axis

μ = $45° - \varphi/2$

$\sigma_1, \sigma_2, \sigma_3$ = principal stresses

σ = $(\sigma_1 + \sigma_3)/2 + \psi$

ω = DB/L (zero subscript indicates initial value)

1. INTRODUCTION

The prediction and analysis of the tractive performance of rigid wheels on soil is one of the basic problems in the field of soil-vehicle mechanics. The soil-wheel interaction theory presented in this paper relates traction performance directly to the strength properties of soil, providing thereby the analytical tool essential for a predictive method. Presentation of the theory and its applications are arranged in this paper in the following order. In Section 2 the theoretical background is presented together with the application of the theory to wheel performance calculations. Section 3 is allocated to the discussion of numerical solution methods. In Section 4, results of experiments are compared with theoretical predictions. In Section 5, results of research work on rigid wheel-soil interaction

are summarized and further development of the theory for application to tire-soil interaction is outlined.

2. THEORETICAL BACKGROUND

The theory of soil-wheel interaction developed at Grumman has been described in detail elsewhere (Ref. 1). The basic concepts of this theory are summarized below for the convenience of reference.

- Calculation of the tractive performance of wheels can always be reduced to the determination of interface stresses. Once these are known, the wheel can be considered as a free body and performance parameters can be determined as resultants of stresses on a free body.
- Soil failure controls the interface stresses beneath a driven rigid wheel. Generally, two soil failure zones are formed beneath wheels, a forward one and a backward one (Fig. 1). The adjectives indicate both the location of these zones relative to the wheel and the direction in which the soil in the failure zones tends to move.
- The geometry of soil failure zones (also called slip line fields) and the associated stresses can be determined by the theory of plasticity for soils.

Interaction between wheel and soil comes into play through the variation of entry and exit angles and through the effect of interface shear stresses on soil reaction. Interface shear stresses, directly related to the applied torque, influence the geometry of failure zones and associated stresses profoundly.

The forward and backward slip line fields are not independent of each other. At their point of junction, the interface normal and shear stresses must be the same for both fields.

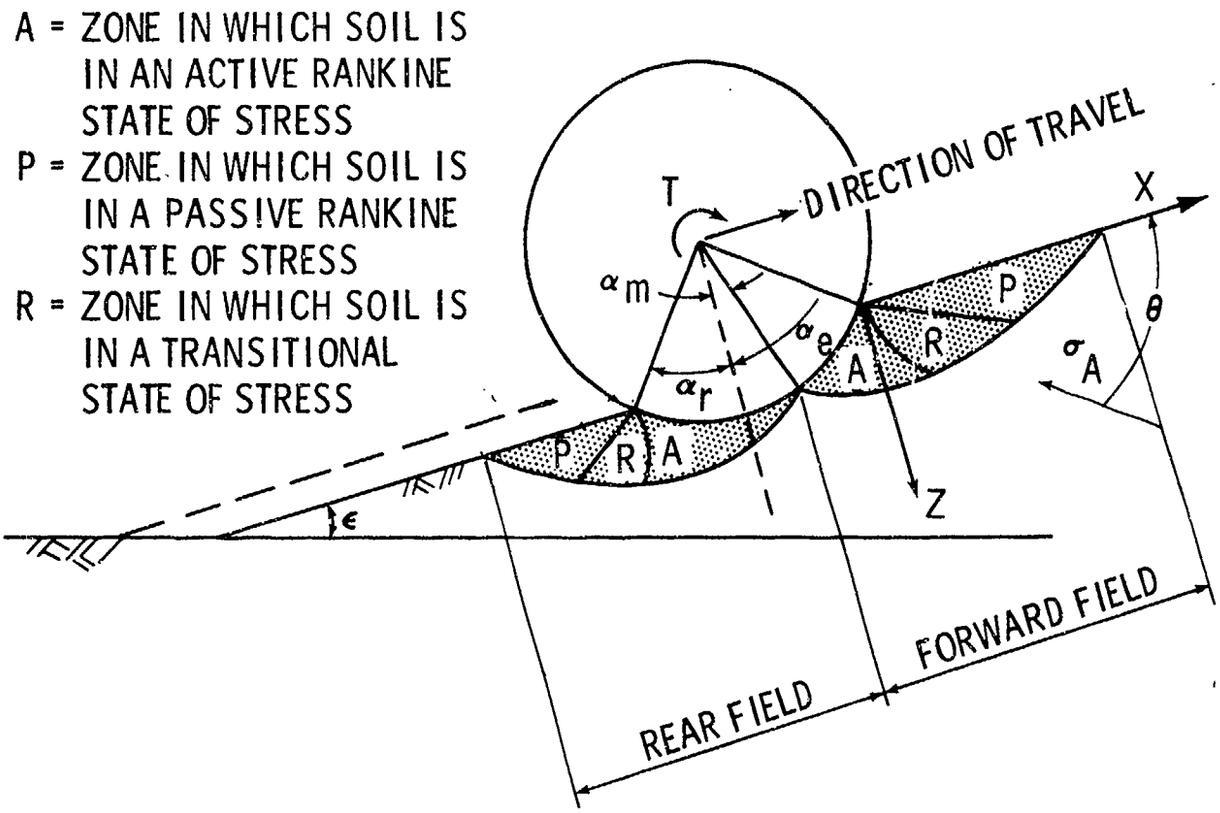

Fig. 1 Definition of Problem Geometry

For the mathematical formulation of the problem, the following assumptions are made:

- The soil is assumed to be semi-infinite, homogeneous, and isotropic.
- Strength properties of the soil are characterized by the cohesion and internal angle of friction.
- Stresses are assumed to be the same in all planes parallel to the plane of motion of the wheel (the problem is assumed to be two dimensional).
- Wheel velocity is constant.
- Soil inertia forces are negligible.
- Soil failure is assumed to be governed by the Mohr-Coulomb yield (failure) criterion as follows:

$$\tau = c + \sigma_n \tan \varphi \quad . \tag{1}$$

- Pore water pressures are negligible.

For these assumptions, the differential equations of plasticity for soils, as derived by Sokolovskii (Ref. 2), are valid and express the geometric and stress conditions that failure zones must meet. These equations are

$$\begin{aligned} dz &= dx \tan(\theta \pm \mu) \\ d\sigma \pm 2\sigma \tan \varphi d\theta &= \frac{\gamma}{\cos \varphi} [\sin(\epsilon \pm \varphi)dx + \cos(\epsilon \pm \varphi)dz] \quad . \end{aligned} \tag{2}$$

For properly defined boundary conditions the above sets of the differential equations of plasticity for soils yield a unique solution in the form of slip line fields and associated stresses. Slip lines represent the orientation of failure surfaces along which the Mohr-Coulomb yield criterion is satisfied, i.e., the

Mohr circle touches the strength envelope. At any point within the slip line field the applicable differential equations set forth above are satisfied.

There are some fundamental aspects of the theory that need to be emphasized here before proceeding with the discussion of the application of the theory to the problem of wheel-soil interaction. These are:

- The Mohr-Coulomb yield criterion as applied in the above equation refers to effective stresses, i.e., for the case where pore water pressures are negligible. (Apparent cohesion due to pore water tension may be considered as effective stress.)
- Equations (2) are valid for a nonlinear strength envelope (Ref. 3) and may be expanded to include pore water pressures (Ref. 4) or soil inertia forces (Ref. 5).
- The Mohr-Coulomb yield criterion implies that the soil strength expressed by Eq. (1) is available regardless of the volumetric strain that is associated with the stress state expressed by Eq. (1). In soil-wheel interaction problems in soft soils, where the soil is progressively compressed as the wheel advances, the volumetric strain in the soil is generally large enough to mobilize the full Mohr-Coulomb strength.
- In plasticity theory, solutions obtained by integration of Eqs. (2) are termed statically admissible solutions and are considered lower bound solutions. Kinematic admissibility is analyzed by constructing velocity fields for the slip zones on the assumption that the material is incompressible. A kinematically admissible

solution would constitute an upper bound. For soil-wheel interaction problems in soft soils the assumption of incompressibility is inappropriate and conclusions drawn on the basis of such an assumption are inapplicable. Experimental evidence, as it will be discussed in Section 4, shows that interface stresses predicted by the application of Eqs. (2) agree reasonably well with measured ones, indicating the validity of the solutions.

Equations (2), with properly defined boundary conditions, yield a unique solution in the form of a slip line field. For the passive zone (Fig. 1), the boundary conditions are completely defined at the free surface. For the active zone, the boundary conditions at the interface constitute a so-called mixed boundary value problem where two of the four variables (x,z,θ,σ) in Eq. (1) have to be specified. In the solution for the conventional bearing capacity problem, z and θ are specified at the base of the bearing plate. In the soil-wheel interaction problem it is not possible to specify a priori the value of any two of the four variables at the interface. Instead, the boundary conditions take the form of a relationship between x and z, given by the wheel geometry and a relationship between θ and the angle of interface friction. This relationship is

$$\theta = \frac{\pi}{2} + \frac{1}{2}(\Delta + \delta) - \alpha \qquad (3)$$

where

$$\Delta = \text{arc sin}\left(\frac{\sin \delta}{\sin \phi}\right) .$$

The interface friction angle, δ, as defined in Fig. 2, establishes a relationship between normal and shear stresses at the interface and represents the degree of mobilization of the soil shear strength at the interface. The orientation of the principal

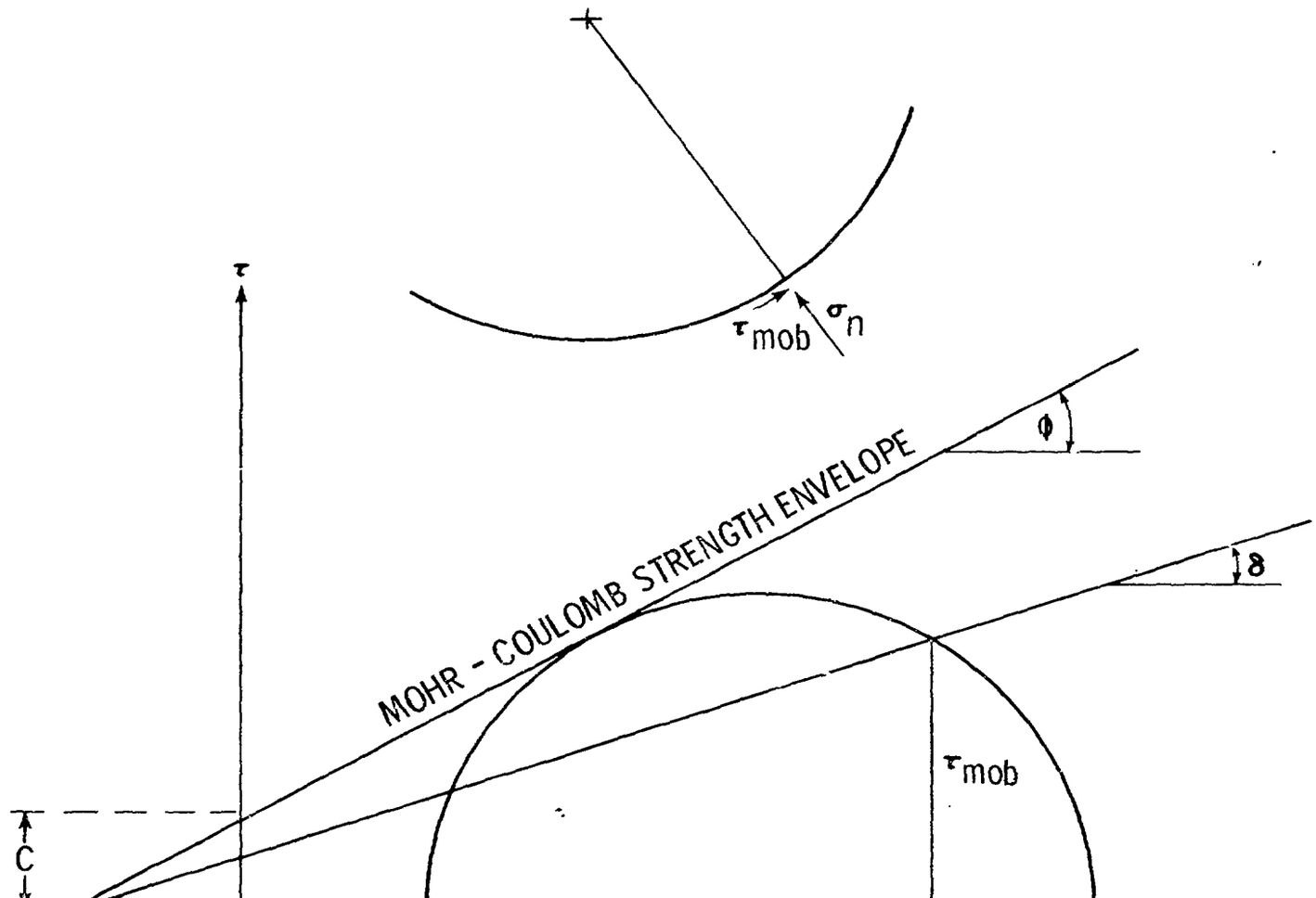

Fig. 2 Mohr Circle, Mobilized Shear Stress and Interface Friction Angle

stresses at the interface, defined by the angle θ, can be computed from Eq. (3) for any given δ angle.

The following relationship holds between the shear strength mobilized at the interface and the angle δ (Fig. 2)

$$\tan \delta = \frac{\tau_{mob}}{\sigma_n + \psi} \quad . \tag{4}$$

The mobilized shear strength is frequently related to slip. On the basis of direct shear tests, Janosi and Hanamoto (Ref. 11) proposed the following relationship between mobilized shear and slip for tracked vehicles:

$$\tau_{mob} = \tau_{max} \left(1 - e^{-j/K}\right) \quad . \tag{5}$$

For compressible soils, which are of primary interest in off-road locomotion, this equation properly describes the relationship between shear stress and slip. When this relationship is applied to the wheel, however, it is useful to include a constant, j_0, in the slip term to account for the fact that there exists a threshold perimeter shear at which movement of the wheel starts. Thus, Eq. (5) is modified as follows:

$$\begin{aligned} \tau_{mob} &= \tau_{max}\left(1 - e^{-(j+j_0)/K}\right) \\ \tan \delta &= \tan \delta_{max}\left(1 - e^{-(j+j_0)/K}\right) \quad . \end{aligned} \tag{6}$$

The concept of soil-wheel interaction as outlined before and shown graphically in Fig. 1 has interesting implications regarding the maximum shear strength (τ_{max}) that can be mobilized at the interface. According to this concept, the soil adjoining the interface is in the active state of failure. For a given normal and

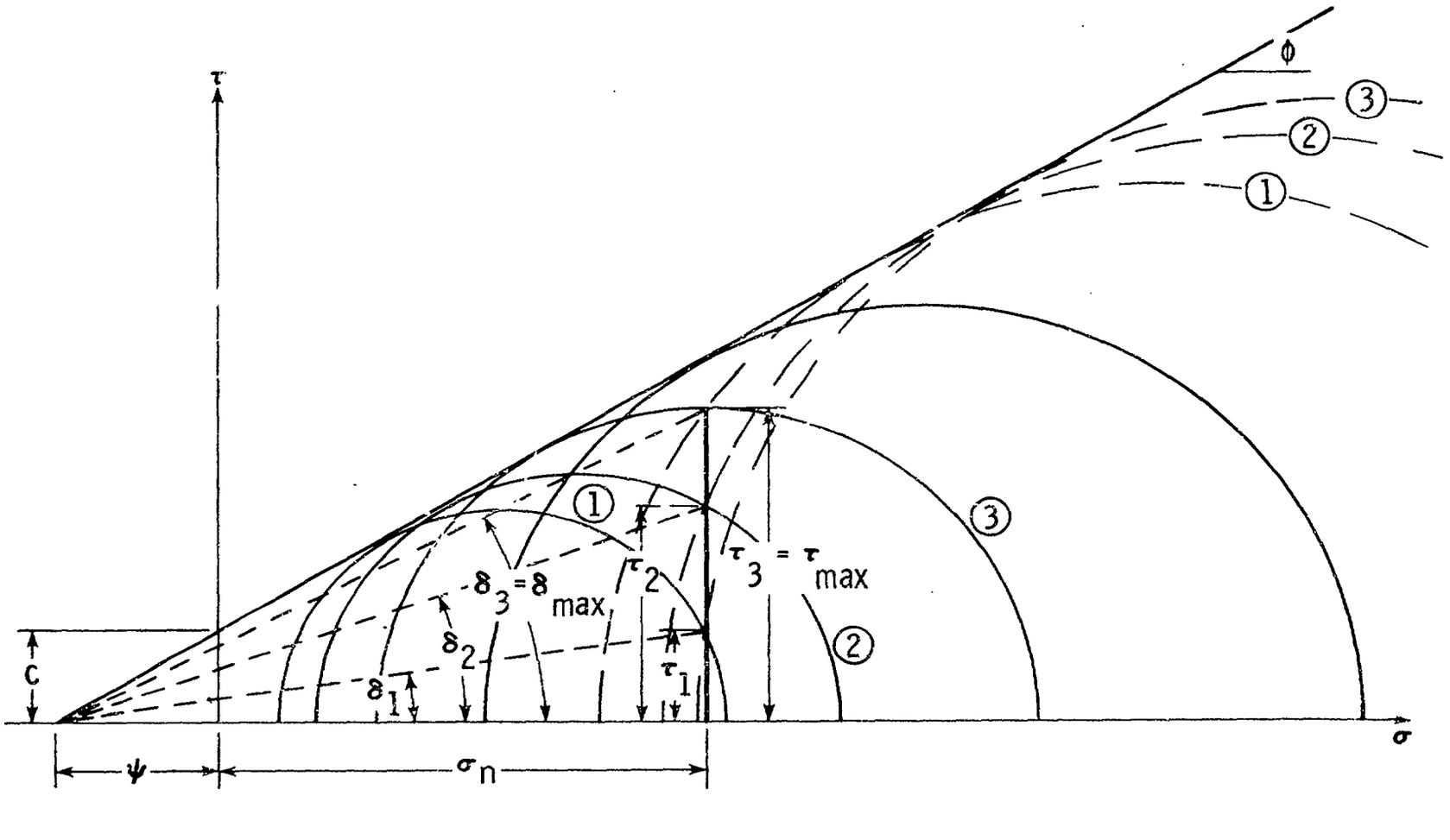

Fig. 3 Development of Shear Stresses at the Interface

shear stress at the interface there is one Mohr circle which represents the active, and another one which represents the passive, states of stresses. Figure 3 shows Mohr circles for the active and passive state for the same normal stress but increasing interface shear stress. Stress circles are shown by full lines for the active state, and by dashed lines for the passive state. The interface shear stress, τ, is shown to increase with the interface friction angle δ ($\tau_3 > \tau_2 > \tau_1$ and $\delta_3 > \delta_2 > \delta_1$). In the active state, the center of Mohr circles is to the left of the shear stress ordinate; in the passive state, it is to the right. From the construction of the Mohr circles, it is obvious that the maximum shear stress that can be mobilized in the active state is the one corresponding to a Mohr circle that has its center at σ_n (circle 3 in Fig. 3). If the shear stress was higher than this, the corresponding Mohr circle would represent a passive state. Thus, it is incorrect to assume that the full soil strength can be mobilized beneath a wheel or track. Passive state can only exist beneath a wheel or track if the soil is pushed toward the wheel or track, an obviously meaningless situation for vehicle mobility. The only possible stress state in the soil beneath a wheel or track is the active state of stresses and it follows from this state that the maximum mobilized shear stress cannot exceed that defined by Mohr circle 3 in Fig. 3. In mathematical terms

$$\tau_{max} = (\sigma_n + \psi) \tan \delta_{max} = (\sigma_n + \psi) \sin \varphi \qquad (7)$$

$$\delta_{max} = \text{arc tan}(\sin \varphi) \quad . \qquad (8)$$

The assumption of interface friction angle defines θ at the interface and together with the geometry defines the boundary conditions so that Eq. (1) yields a unique solution for the slip line

field geometry and associated stresses. For the soil-wheel interaction problem, however, the boundary conditions for both the forward and rear slip line fields have to be defined so that the solution is unique. This involves the determination of angle α_m that separates the forward and rear fields. The following considerations apply in this respect.

For dry sand it was found by Sela (Ref. 6) that the angle of separation equals the developed friction angle. This finding is consistent with the concept that the forward failure zone extends over that part of the wheel perimeter where the component of the normal and shear stresses, (ΔD), in the direction of motion is negative (i.e., resisting the motion), and the backward zone extends over that part of the wheel perimeter where this component is positive. Applying this concept to soils with cohesion results in the following relations

$$\Delta D = \tau_{mob} \cos \alpha - \sigma_n \sin \alpha$$

$$\Delta D = (\sigma_n + \psi) \tan \delta \cos \alpha - (\sigma_n) \sin \alpha = 0 \qquad (9)$$

$$\alpha_m = \arctan \left(\frac{\sigma_n + \psi}{\sigma_n} \tan \delta \right) .$$

3. TECHNIQUES OF NUMERICAL SOLUTIONS

The calculation of wheel performance on the basis of the concepts described in the preceding section involves the following steps:

- For given wheel size, soil strength properties, and interface friction parameter (or slip), computation of the geometry of a single slip line field and the associated stresses by numerical methods.

Security Classification

DOCUMENT CONTROL DATA - R & D

(Security classification of title, body of abstract and indexing annotation must be entered when the overall report is classified)

1. ORIGINATING ACTIVITY (Corporate author)	2a. REPORT SECURITY CLASSIFICATION
Grumman Aerospace Corporation	U
	2b. GROUP

3. REPORT TITLE

Tractive Performance of Wheels in Soft Soils

4. DESCRIPTIVE NOTES (Type of report and inclusive dates)

Research Report

5. AUTHOR(S) (First name, middle initial, last name)

Karafiath, L.L. and Nowatzki, E.A.

6. REPORT DATE	7a. TOTAL NO. OF PAGES	7b. NO. OF REFS
February 1973	40	11

8a. CONTRACT OR GRANT NO.	9a. ORIGINATOR'S REPORT NUMBER(S)
b. PROJECT NO.	RE-443J
c.	9b. OTHER REPORT NO(S) (Any other numbers that may be assigned this report)
d. N/A	N/A

10. DISTRIBUTION STATEMENT

Approved for public release; distribution unlimited.

11. SUPPLEMENTARY NOTES	12. SPONSORING MILITARY ACTIVITY

13. ABSTRACT

The traction developed by a wheel can be determined by appropriate integration of the soil wheel interface stresses. In soft soils these are governed by failure conditions in the soil brought about by the wheel load. The geometry of the two failure zones (front and rear), as well as the associated stresses, are computed by solving the differential equations of plasticity by numerical techniques. A flow diagram shows the computation of failure zones and associated interface stresses that yield the load, torque and traction for a given wheel geometry and interface friction. Slip-shear stress equations are used to relate interface friction to slip. The solution of the practical problem of determining traction and slip for given soil conditions and applied wheel load and torque requires an iteration procedure that is shown in another flow diagram. Inputs for the computer program are soil properties, wheel load, and torque; the end outputs are traction slip and sinkage. For the computation of traction exerted by tires, a soil-tire model has been developed that allows for the deflection of the tire and attendant restraint of the normal interface stresses.

DD FORM 1 NOV 65 1473

U

Security Classification

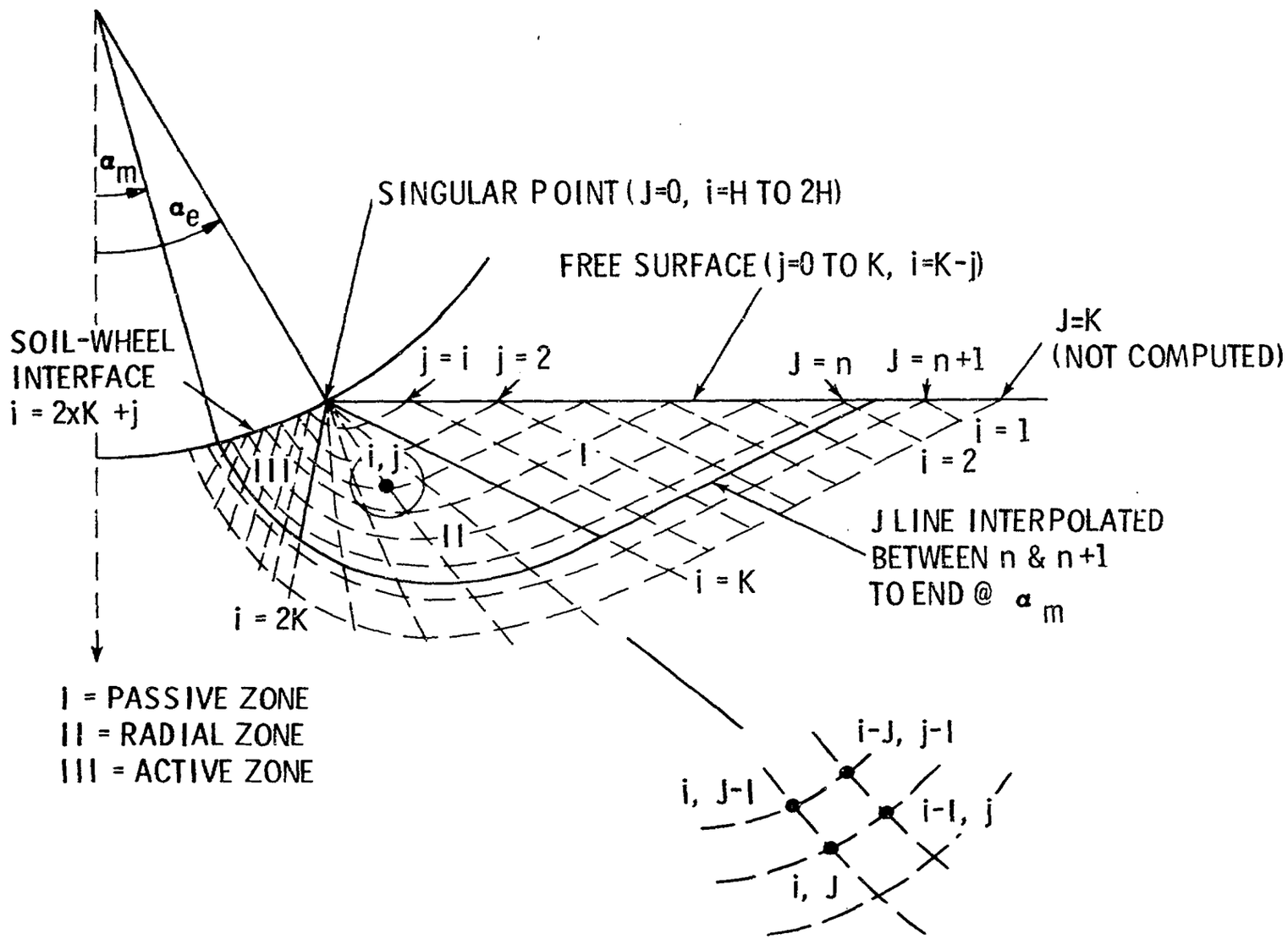

Fig. 4 Computation of Slip Line Field by Finite Differences

- Determination of a matching set of forward and rear slip line fields and the corresponding load, torque, and drawbar pull (or drag).
- Inversion procedure to find torque and slip for given load and drawbar pull or drawbar pull and slip for given load and torque.

3.1 For the computation of a single slip line field, finite difference forms of Eqs. (2) are used. These forms allow the computation of variables at a point (i,j) from their values at points (i-1,j) and (i,j-1) (Fig. 4). The procedure is described elsewhere in detail (Refs. 7 and 8) for the case of bearing capacity computations. For the problem of soil-wheel interaction it is more convenient to employ a different sequence of operations. Instead of computing the variables first in the passive, then in the radial, and finally in the active zone, the variables are computed along the first "j" line in all three zones and then along subsequent "j" lines until a "j" line ends at a point at the interface past the angle of separation. A "j" line is then interpolated between this and the previous "j" line so that it ends up at α_m within a preassigned limit of tolerance (ξ). This method eliminates the time consuming trial and error procedure of finding the length of passive zone that matches the arc length of the active zone. The length of the passive zone in this procedure is overestimated so that the last j line would overshoot the α_m angle.

The grid in this procedure is larger than in the conventional one (say 16 x 48 instead of 10 x 30) requiring a somewhat larger computer core, but the computing time for finding a slip line field that meets the boundary conditions at α is much less.

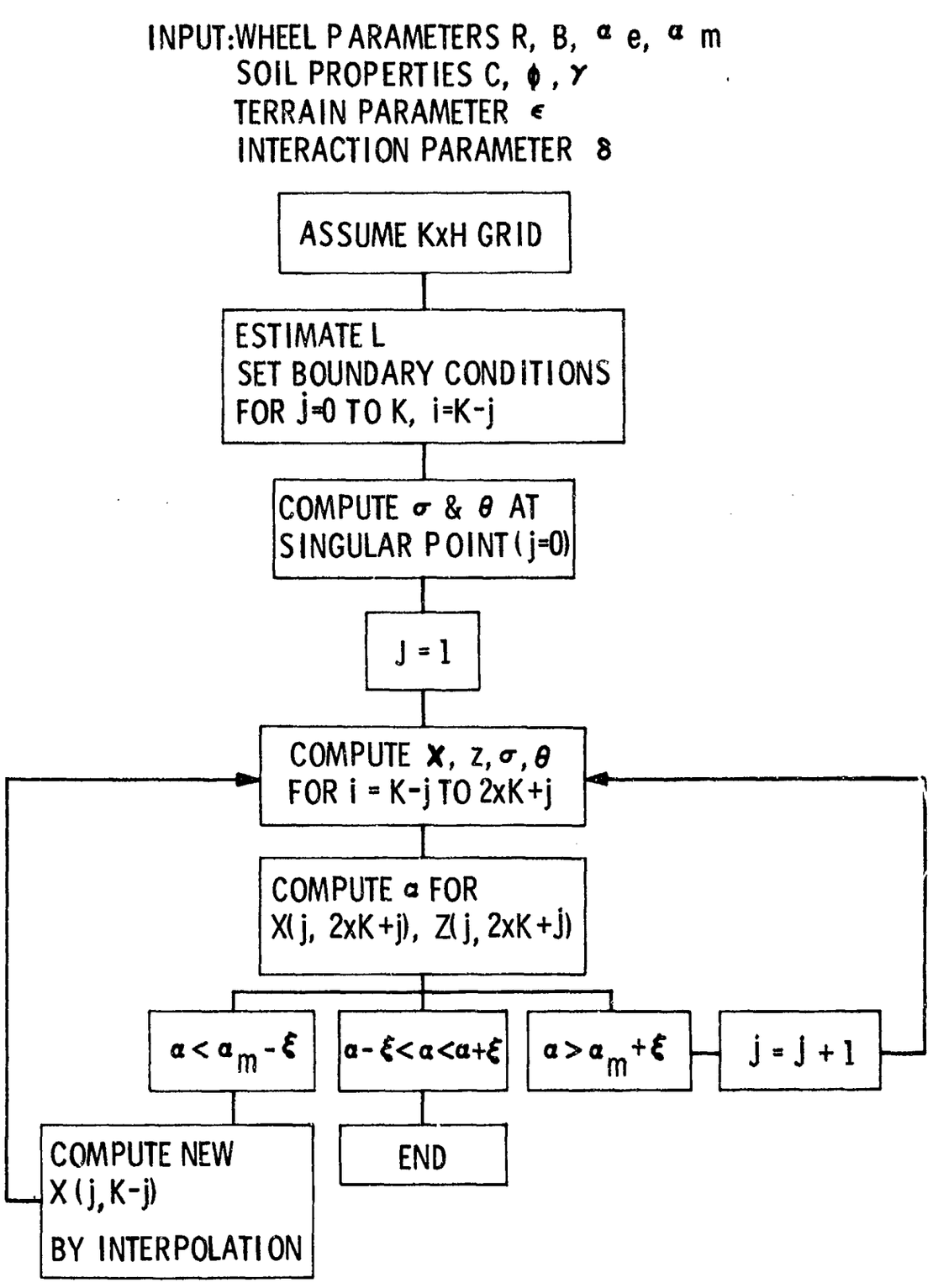

Fig. 5 Flow Diagram for the Computation of a Single Slip Line Field

The procedure for the computation of a single slip line field is described in the flow diagram shown in Fig. 5. The interface friction angle, as shown in the flow diagram, is assumed to be constant. However, the program can also accommodate a δ angle which varies along the interface.

3.2 The computation of a matching set of slip line fields starts with the rear slip line field using the subroutine outlined in 3.1, but allowing for appropriate sign changes due to the fact that the rear field is a mirror image of the front field. The reason for starting the computation with the rear field is two-fold: first, the rear angle varies within a narrow range; secondly, a normal stress from the rear field (q_{mr}), at α_m, can be generally matched by a forward field. This is not true vice-versa. When q_{mr} for the assumed rear angle (α_r) and interface friction angle (δ) is determined, the front field is found by varying the entry angle (α_e) until the normal stress from the front field (q_{mf}) matches q_{mr} within the allowed tolerance. Since the interface friction angle δ is assumed to be the same for both the forward and rear fields, the shear stress at α_m from both fields is the same (within the tolerance) when q_{mr} and q_{mf} are matched. When a matching set of rear and forward fields is found by this procedure the load, torque, and drawbar pull is computed by appropriate numerical integration of the interface stresses. The slip is computed from Eq. (6) and the sinkage from the entry angle. The flow diagram for the computation of a matching set of slip line fields is shown in Fig. 6.

3.3 In many cases the problem is posed differently and it is necessary to solve for torque, slip, and sinkage for given wheel load, drawbar pull, and soil properties. In the solution procedure outlined in 3.2, load, drawbar pull, and torque are functions of the

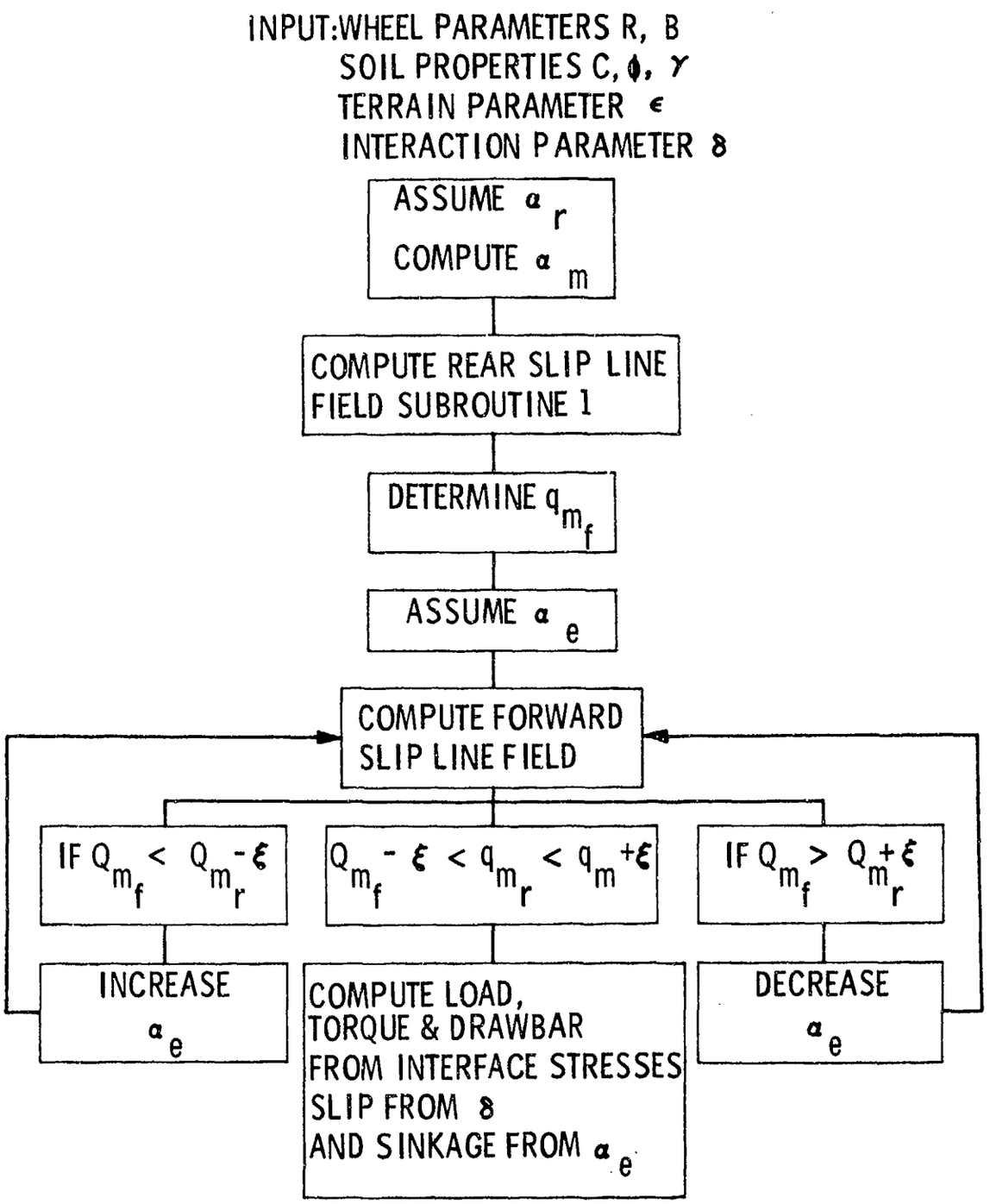

Fig. 6 Flow Diagram for the Computation of a Matching Set of Slip Line Fields and Wheel Performance Parameters

rear angle α_r, and interface friction angle δ, as expressed by the following relationship

$$L = f_1(\alpha_r, \delta)$$

$$DB = f_2(\alpha_r, \delta) \qquad (10)$$

$$T = f_3(\alpha_r, \delta) \quad .$$

The functions f_1, f_2, f_3 are, of course, not closed form functions, and in the solution procedure outlined in 3.2, one set of L, DB, T values are found for an assumed α_r and slip corresponding to an assumed δ. The procedure to find the torque for given load and drawbar pull consists of finding α_r and δ which yield the load and drawbar pull; once the matching set of slip line fields for these conditions is found, the torque, slip, and sinkage is also available from the computations. Even if the functions f_1 and f_2 were known, the solution for L and DB would require the solution of a system of two nonlinear equations. Since there is no generally valid theorem for the solution of this problem and convergence criteria for iterative solutions can not be established if the derivatives of f_1 and f_2 are not known, it was necessary to study the general behavior of these functions and make judicious use of some of their properties to devise an efficient convergent iteration scheme for the solution of the problem.

The general behavior of the load and drawbar pull as functions of α_r and δ is illustrated in Figs. 7 and 8, where isometric views of computed L and DB values are shown for the following input parameters:

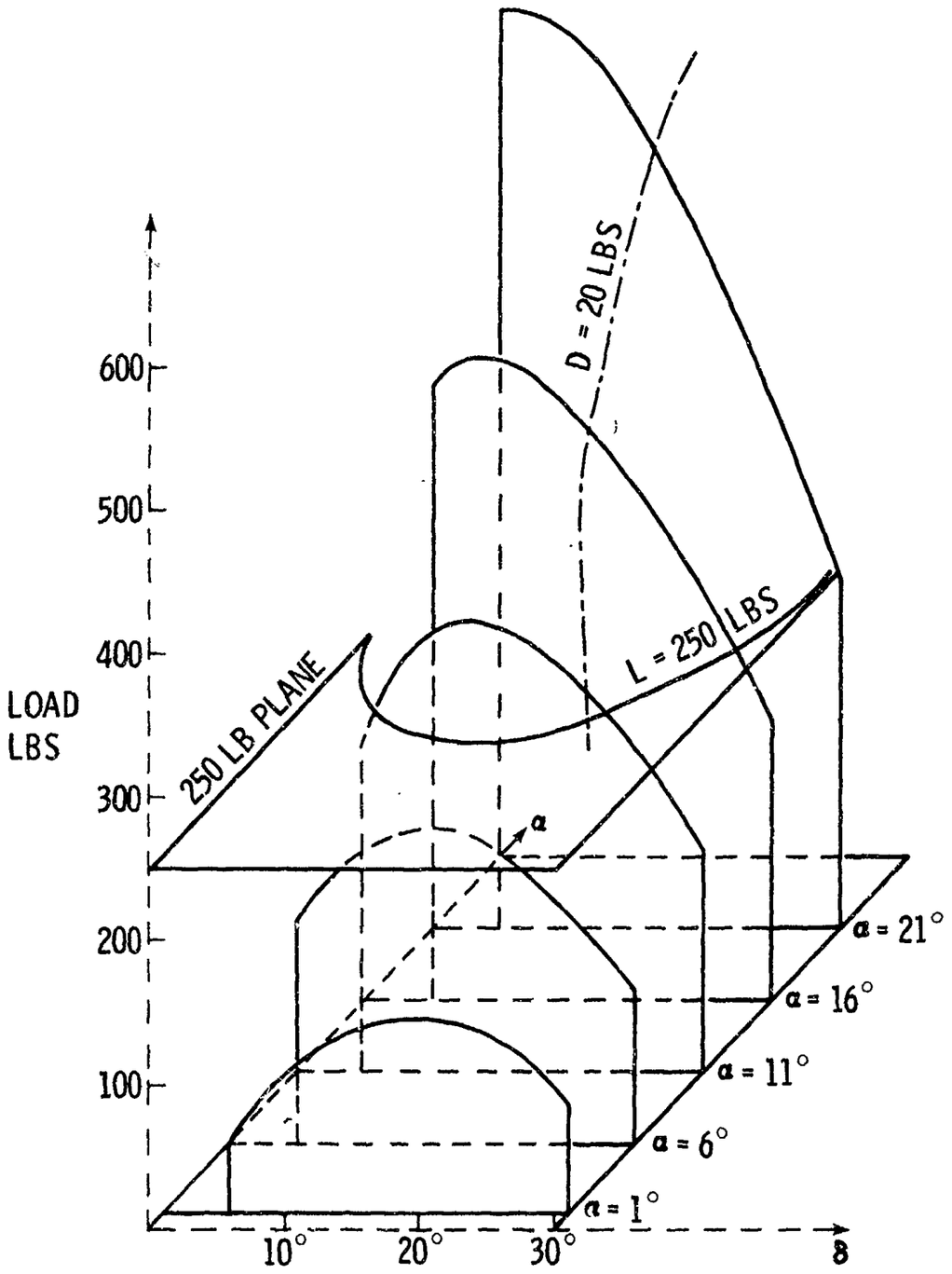

Fig. 7 Isometric View of the Function $L = f(\alpha, \delta)$

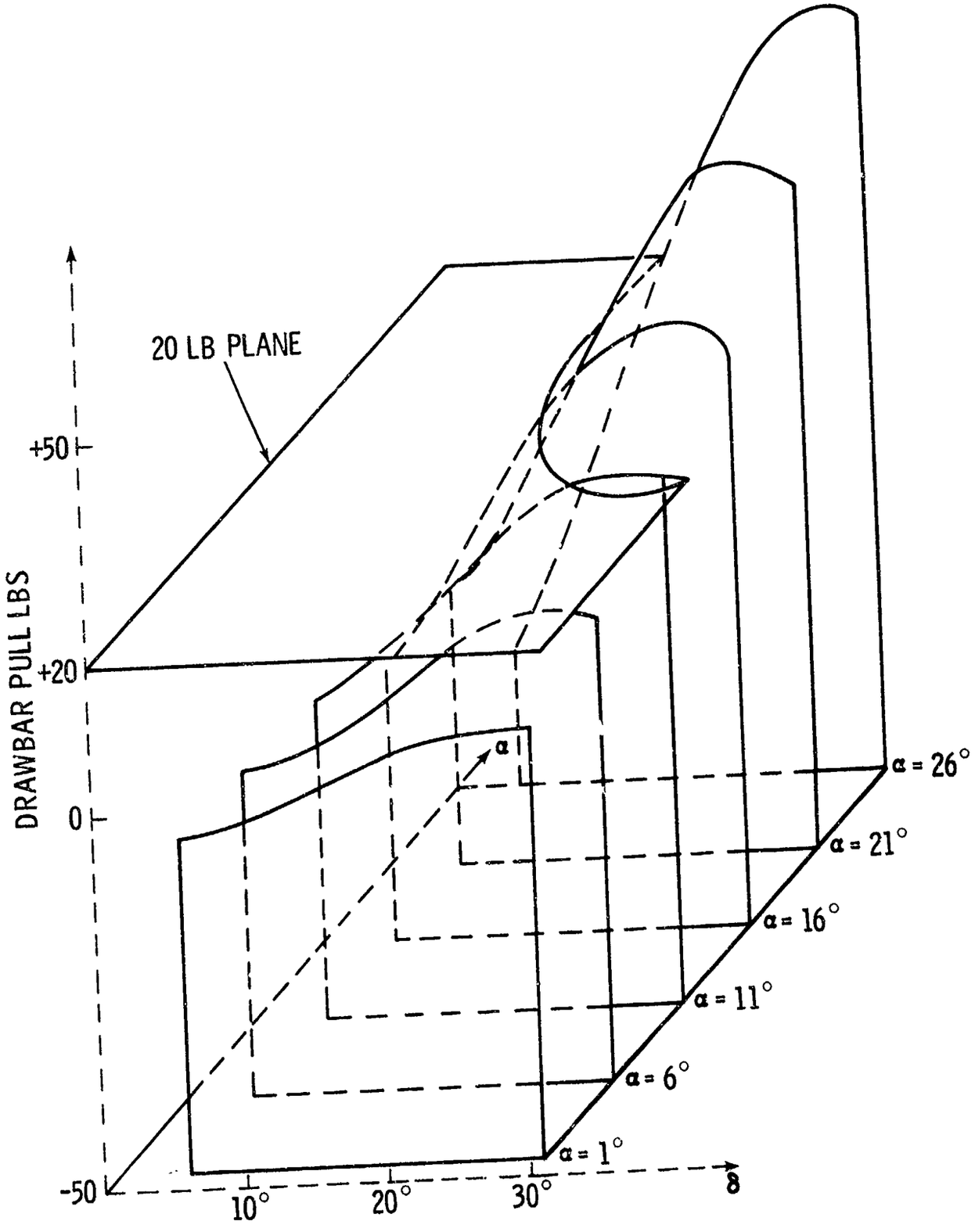

Fig. 8 Isometric View of the Function $D = f(\alpha, \delta)$

wheel radius		1.15 ft
wheel width		0.36 ft
Forward field	friction angle	38°
	unit weight	100 lbs/cu ft
Rear field	friction angle	41°
	unit weight	110 lbs/cu ft

The problem of finding the α and δ values for given L (250 lbs) and DB (20 lbs) is also illustrated in these figures. The contour line marked L = 250 lbs in Fig. 7 represents all combinations of the α_r and δ values that result in that load, while the contour line marked DB = 20 lbs in Fig. 8 represent all combinations of α_r and δ that yield 20 lbs drawbar pull. The intersection of this latter contour line (replotted in Fig. 7 by dash-dot line) with the L = 250 lbs contour line yields the unique solution.

The surfaces representing the variation of L and DB with α_r and δ, shown in Figs. 7 and 8, indicate that iteration procedures based on linear approximations are not likely to succeed. Further study of the relationships between these variables indicated, however, that, in general, L monotonically increases with α_r, and the ratio DB/L (pull coefficient) monotonically increases with δ. These features allowed the development of the iteration scheme shown in Fig. 9. This iteration scheme is the basis of the computer program, developed for the U.S. ATAC, which computes torque, slip, and sinkage for given soil properties, wheel load, and drawbar pull. The program requires a 9K core and average computer time is in the range of 30-60 seconds on a PDP 10 computer.

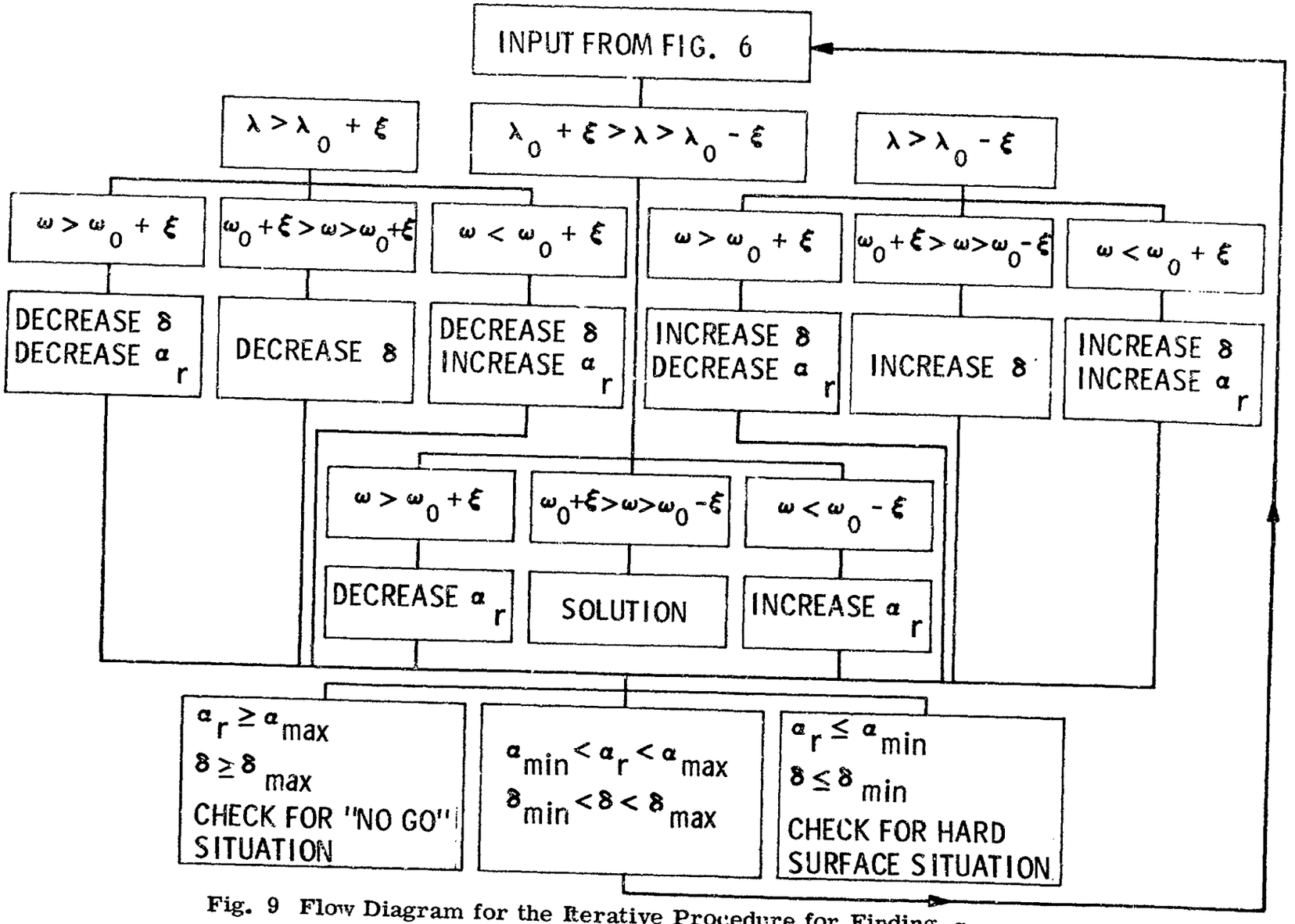

Fig. 9 Flow Diagram for the Iterative Procedure for Finding α_r and δ Values for Given Load, Drawbar Pull and Soil Properties

4. EXPERIMENTAL RESULTS

In the development of the theory, utmost attention was paid to the experimental information that was available at that time on the stress state in the soil and at the soil-wheel interface. Comparative discussions of these experimental results with the theory are given in Refs. 1, 3, and 4.

In the spring and summer of 1972 a validation test series, sponsored by the U.S. ATAC was conducted at the Stevens Institute of Technology. In this test series a 1.15 ft diameter, 0.36 ft wide wheel was instrumented to measure the interface normal and shear stresses at four locations, evenly distributed between the centerline and edge of the wheel. The tests were performed in both loose and dense sand and in a light clay (loam) at various loads and slips. The strength properties of the soil were determined by triaxial tests; cone penetrometer tests were performed before and after the wheel tests to obtain information on the actual density of the soil bed. Typical results of these experiments are given below; detailed results of the entire program will be presented in the final report on U.S. Army Tank Automotive Command, Contract No. DAAE 07-72-C-0033.

4.1 Loose sand. The friction angle of the loose sand, has been determined by triaxial tests as $\phi = 38°$. In the rear field, however, cone penetrometer tests indicated a considerable increase in the density. The friction angle corresponding to the increased density was found to be $\phi = 41°$.

Fig. 10 shows both the measured and computed distribution of average normal and shear stresses at the interface for 33 percent slip; Fig. 11 for 22 percent slip, and Fig. 12 for 13 percent slip. The computed and measured load, torque, and drawbar pull

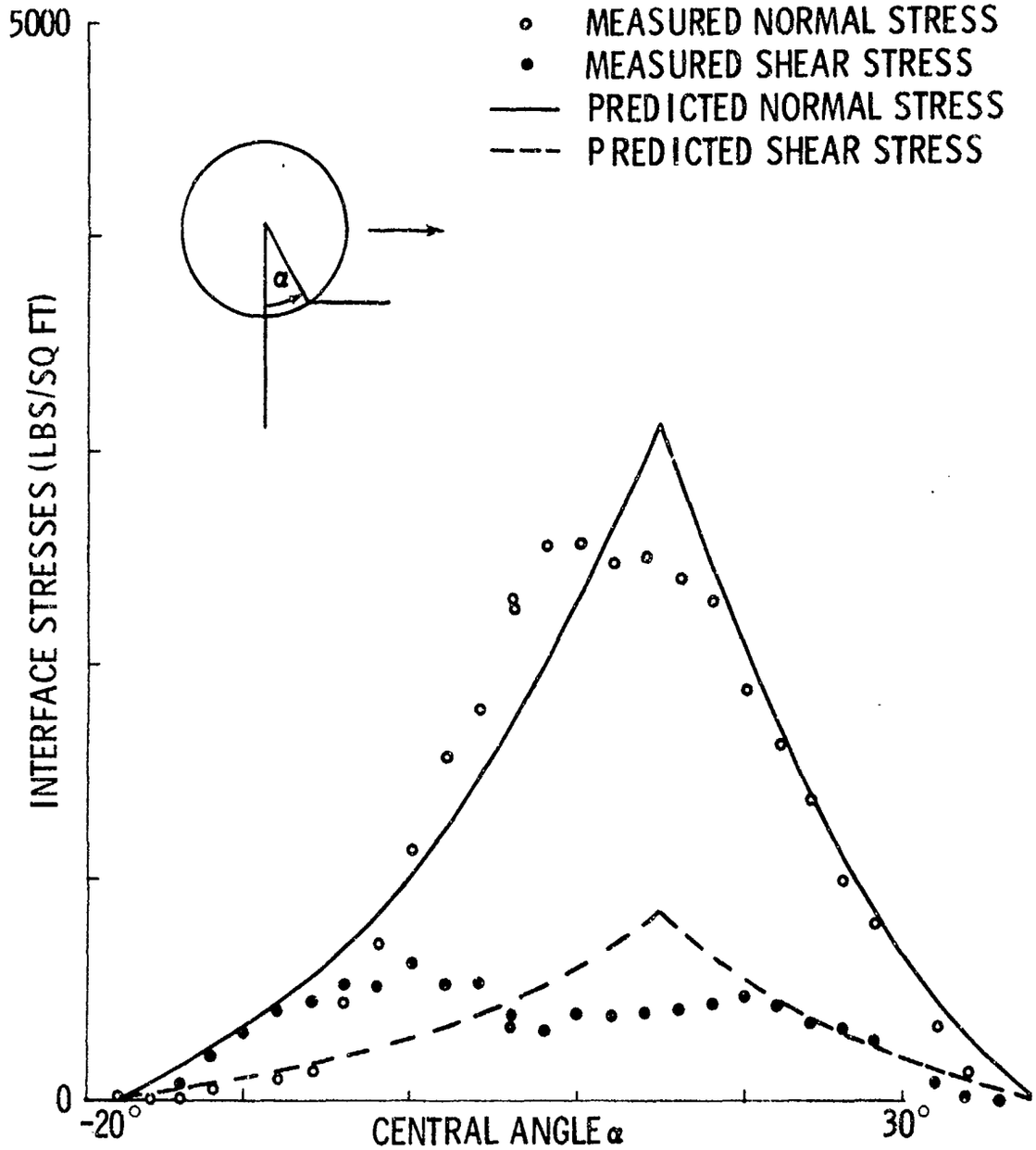

Fig. 10 Comparison of Measured and Computed Interface Stresses for a 1.15 ft Diameter, 0.36 ft Wide Driven Wheel in Sand (33% Slip). Run #102.

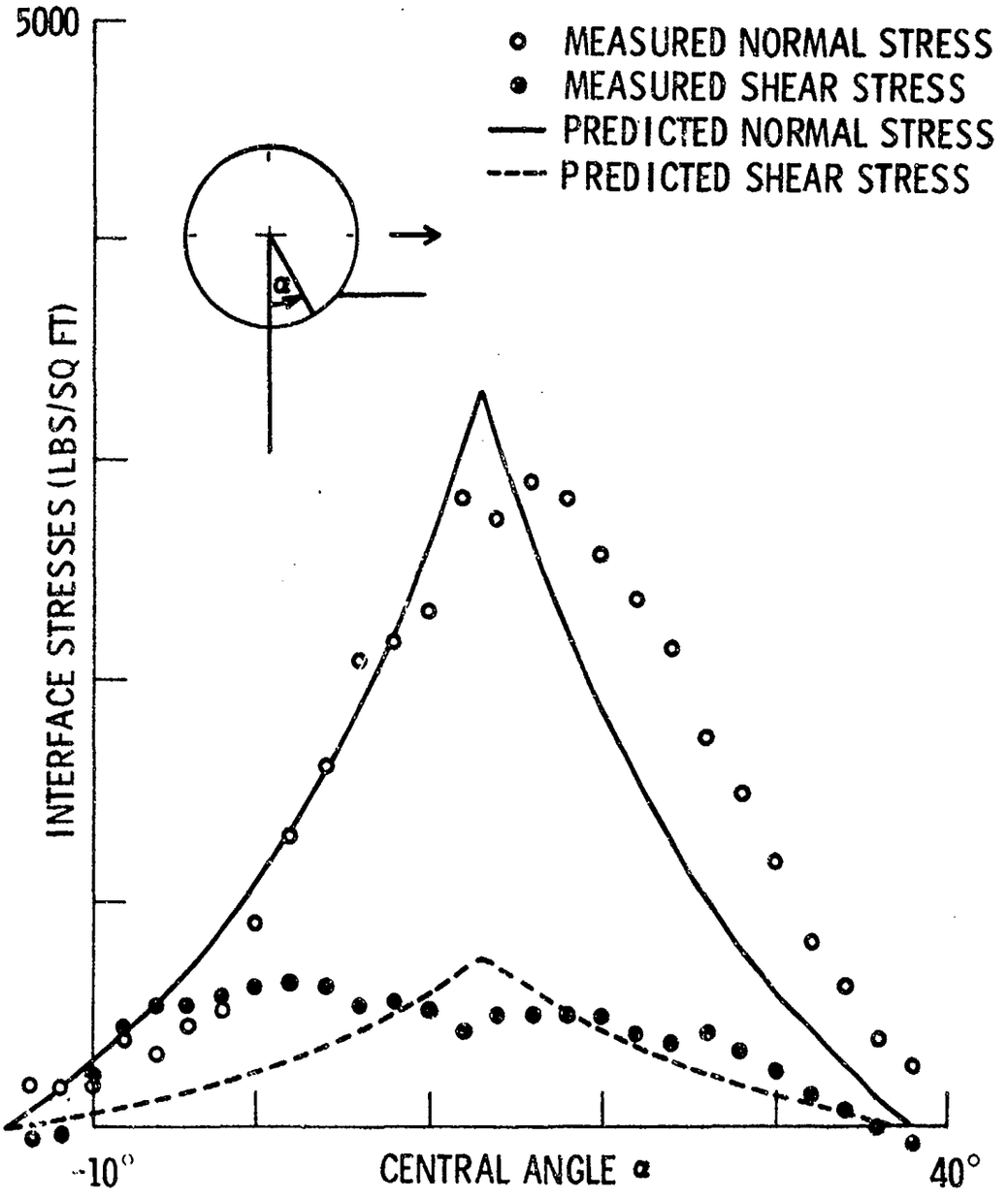

Fig. 11 Comparison of Measured and Computed Interface Stresses for a 1.15 ft Diameter, 0.36 ft Wide Driven Wheel in Sand (22% Slip). Run #105.

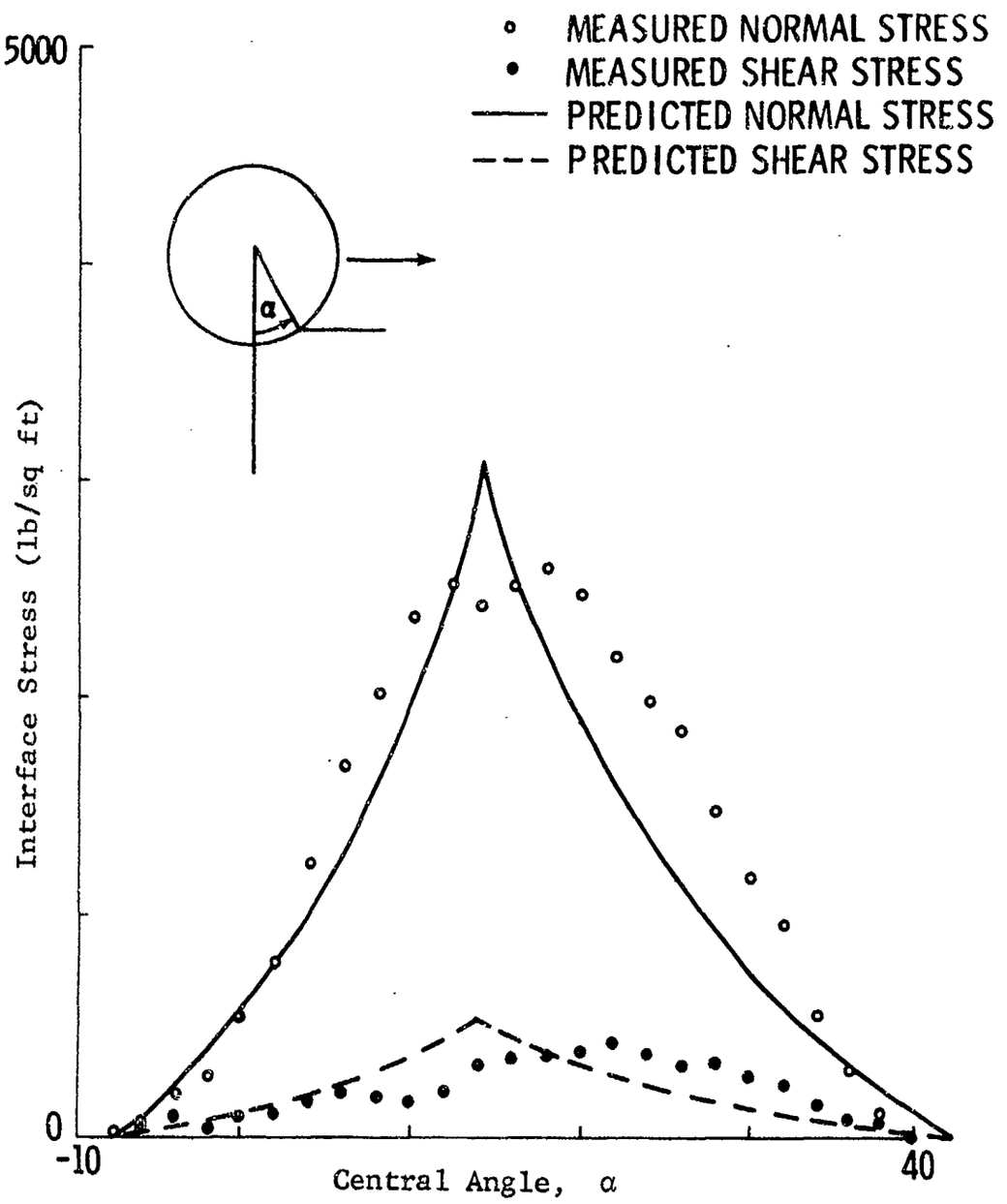

Fig. 12 Comparison of Measured and Computed Interface Stresses for a 1.15 ft Diameter, 0.36 ft Wide Driven Wheel in Sand (13% Slip). Run #40.

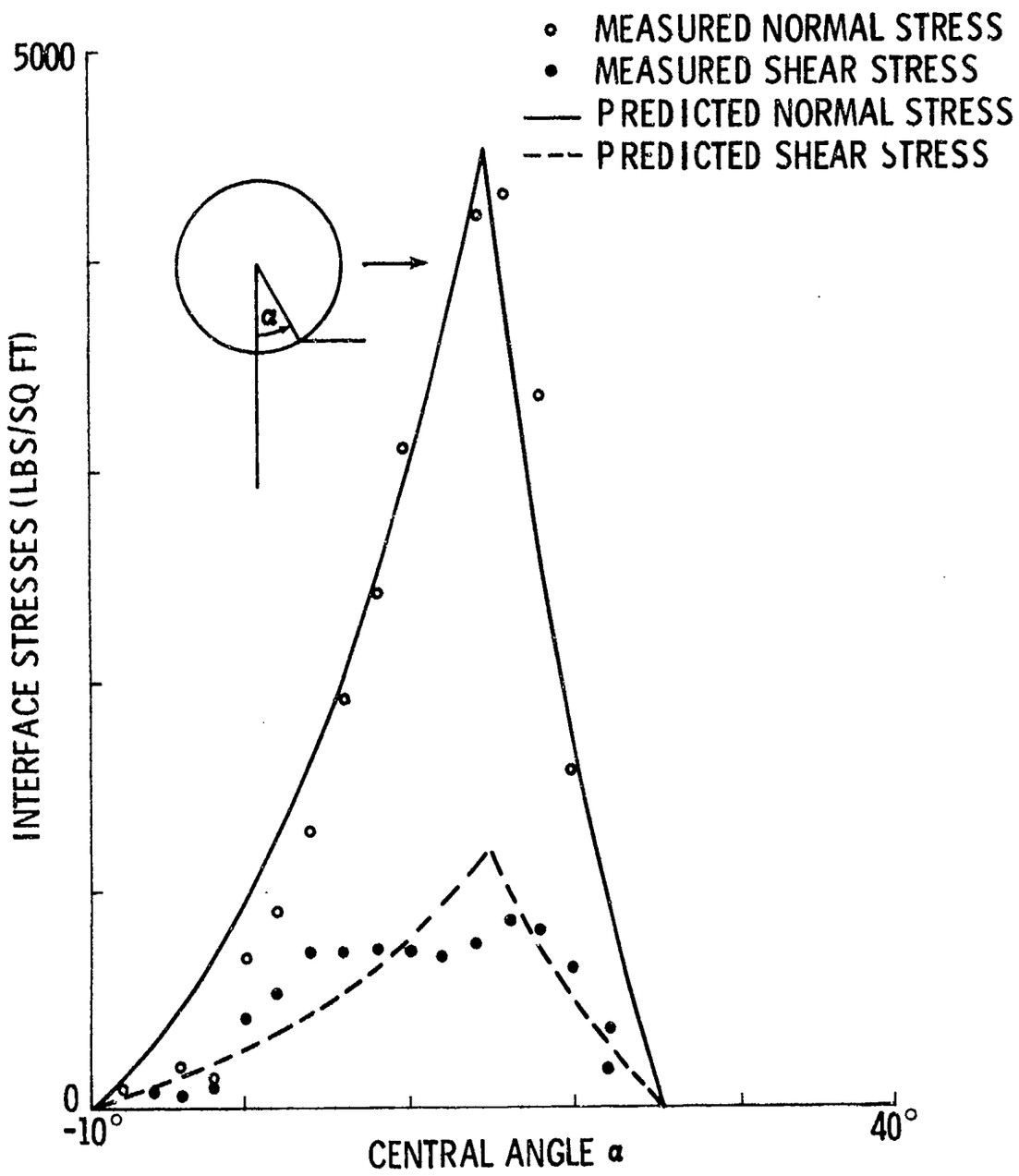

Fig. 13 Comparison of Measured and Computed Interface Stresses for a 1.15 ft Diameter, 0.36 ft Wide Driven Wheel in Sand (28% Slip). Run #98.

values are shown in Table 1. The constants in the slip relation, Eq. (6), were determined from the actual wheel performance tests as $j_o = 0.098$ and $K = 0.76$. Further research is needed to determine whether these constants are generally valid for cohesionless soils and other wheel dimensions.

4.2 Dense sand. In this test series the sand was compacted by vibration. For this condition the friction angle was found to be $\phi = 44°$. Cone penetrometer tests indicated that wheel passage actually loosened the sand. Since this loosening is the end result of the shearing process, the same friction angle was used for the rear field as in the front. Interface stresses obtained in a typical test are shown in Fig. 13 and pertinent data are shown in Table 1. The slip for the dense sand was computed by the constants determined for loose sand; the constants appear to be valid for both cases.

4.3 Loam (light clay). For this test series the loam bed was prepared at about 16 percent moisture content and lightly rolled to provide a uniform surface. Strength properties of this soil were also determined by triaxial tests performed at a loading rate comparable to that in the wheel performance tests. Cone penetrometer tests were conducted before and after the wheel passage and also in small soil bins where placement and moisture was well controlled. These tests served the purpose of correlating triaxial test results and actual conditions in the test bed.

Figure 14 shows actual measurements from three runs performed under the same conditions and the computed stresses for $C = 130$ lbs/sq ft, and $\phi = 23°$ in the front field, and $C = 195$ lbs/sq ft, and $\phi = 20.7°$ in the rear field. The interface stress measurements for the three runs are almost identical indicating the reproducibility of the results. The computed stresses

Table 1

COMPARISON OF MEASURED AND COMPUTED WHEEL PERFORMANCE PARAMETERS

Run No.	Wheel Dia, ft	Wheel Width, ft	Soil		Load, lbs	Drawbar Pull, lbs	Torque, lbs/ft	Slip, Percent
102	1.15	0.36	Loose Sand	Measured	444	24	144	33
				Computed	484	19	147	33
105	"	"	"	Measured	532	2	164	22
				Computed	482	5	127	26
40	"	"	"	Measured	462	-54	94	13
				Computed	400	-41	81	13
98	"	"	Compacted Sand	Measured	426	32	138	28
				Computed	457	37	137	28
140-142	"	"	Loam	Measured	489	33	141	- 6
				Computed	482	14	124	- 6
110102 (Level)	0.3334	0.1667	Jones Beach Sand	Measured	7.5	1.22	0.67	17
				Computed	7.2	1.8	0.8	21
110602 (Slope)	"	"	Jones Beach Sand	Measured	10.7	0.81	0.82	17
				Computed	8.9	1.1	1.0	21

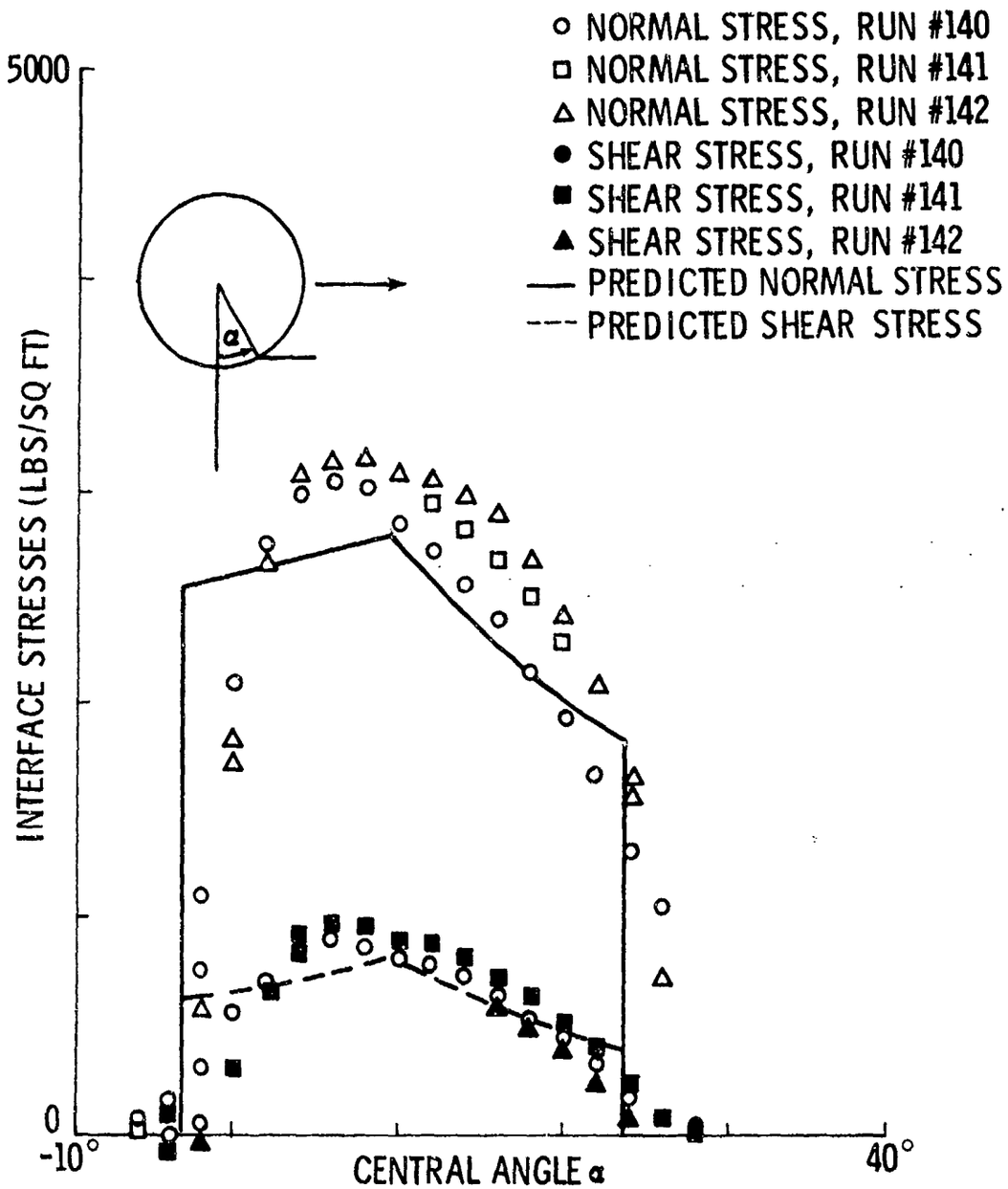

Fig. 14 Comparison of Measured and Computed Interface Stresses for a 1.15 ft Diameter, 0.36 ft Wide Driven Wheel in Clay (-6% Slip). Run #140-142.

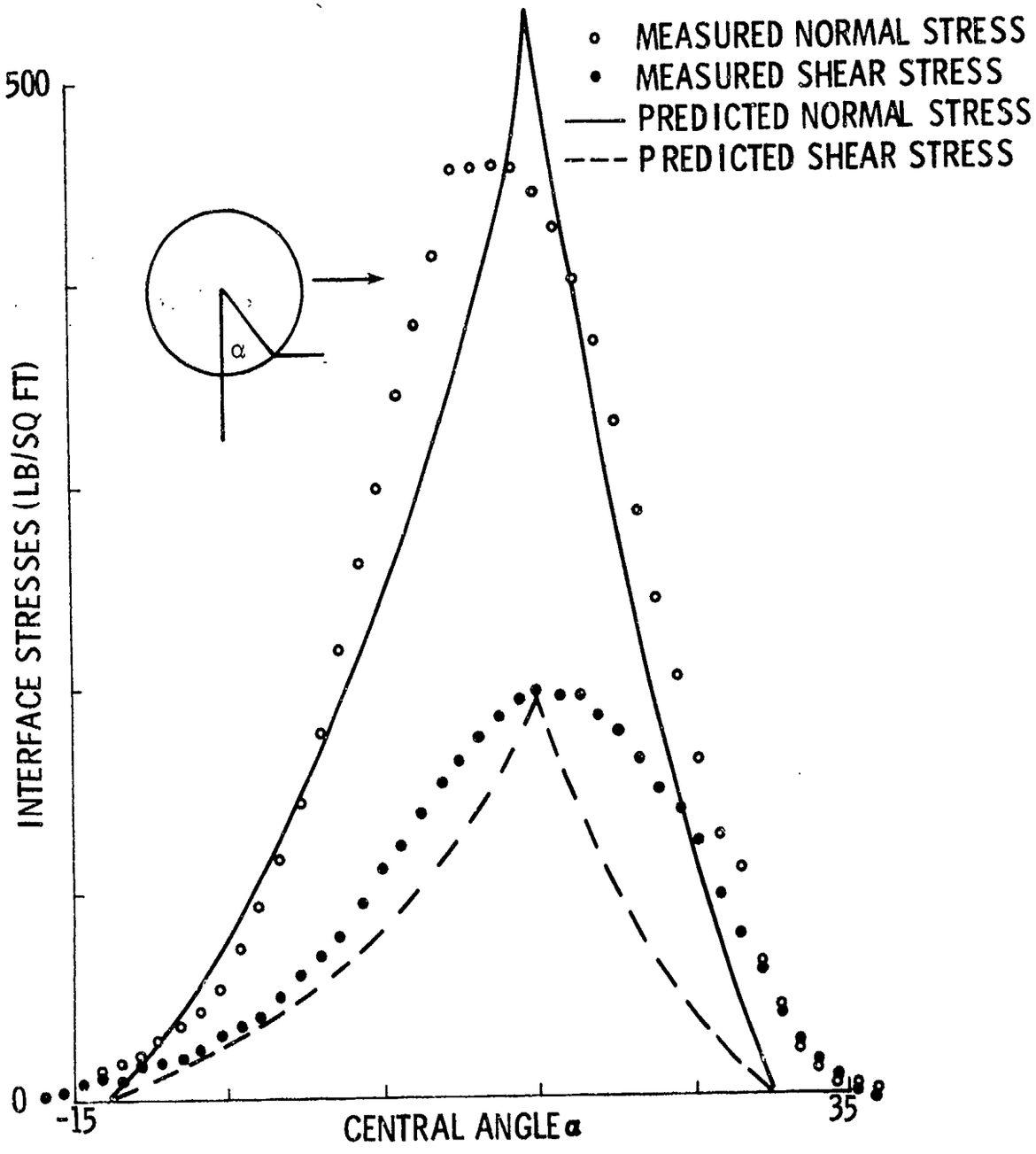

Fig. 15 Comparison of Measured and Computed Interface Stresses for an 8-in Diameter, 2-in Wide Driven Wheel in Jones Beach Sand-Bin Sloped 4° (17% Slip). Run #110602.

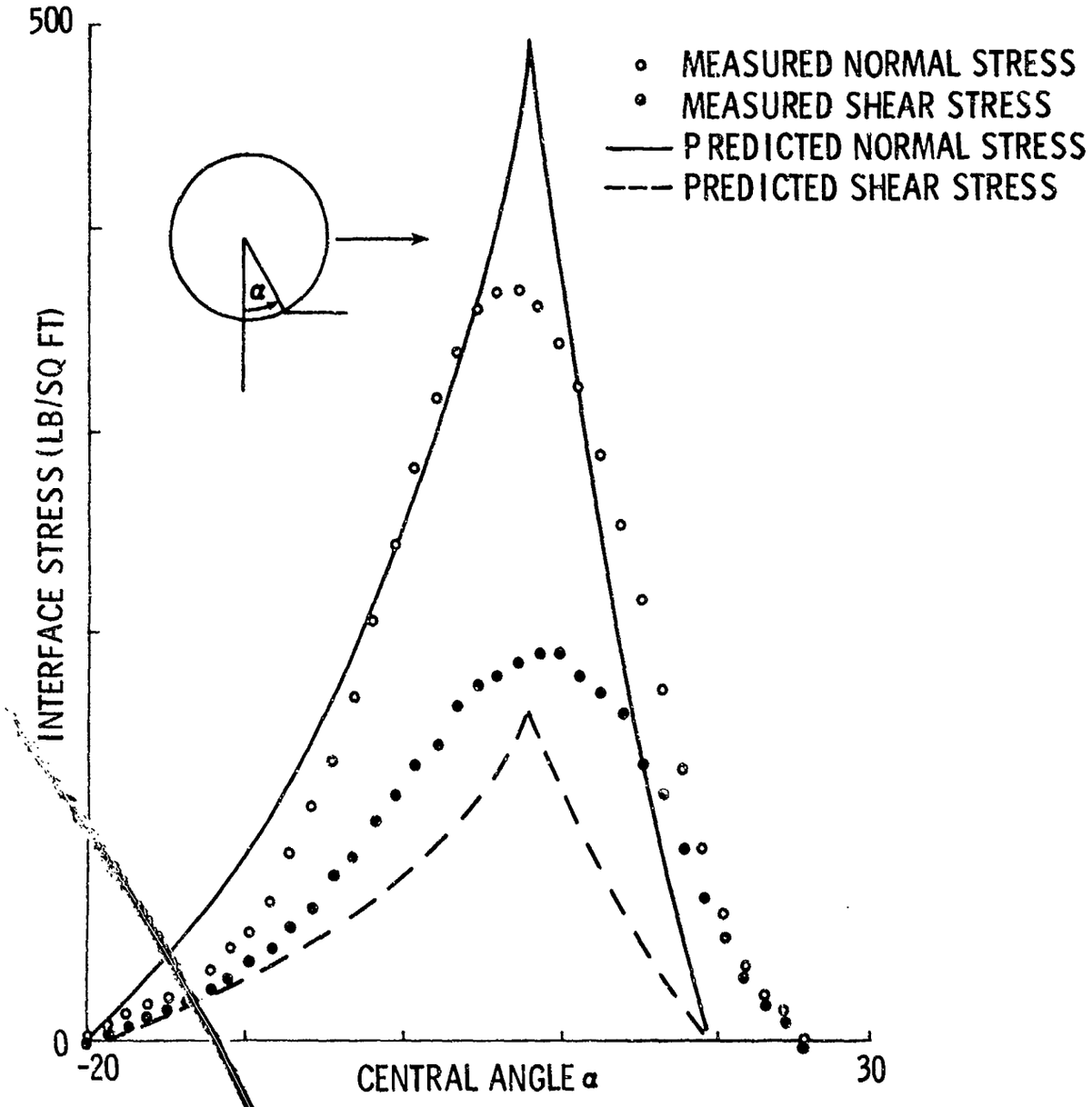

Fig. 16 Comparison of Measured and Computed Interface Stresses for an 8-in Diameter, 2-in Wide Driven Wheel to Jones Beach Sand - Bin Level (17% Slip). Run No. 110102

duplicate the measured ones quite closely, although in the experiments the stresses never rise instantaneously, as predicted by theory. The slip coefficients established for the loam are $j_o = 0.089$ and $K = 0.09$, substantially different from those for sand. Computed and measured wheel performance parameters are shown in Table 1.

4.4 Another series of validation tests using a smaller sized bin and wheel was conducted at Grumman. In this test series, an 8-inch diameter, 2-inch wide, wheel was instrumented to measure interface normal and shear stresses at the centerline and then at the edge of the wheel. The bed material was medium dense Jones Beach sand whose properties had been previously determined and reported (Refs. 7 and 9). The tests were performed for various loads at slips ranging from 9 percent drag to 39 percent slip. Friction angle in the forward zone was 36 degrees and in the rear zone 41 degrees based on results of triaxial and cone penetrometer tests. The bin at Grumman possesses the unique capability of providing a slope up which the wheel may be driven or pulled. Therefore, the effects of slope on wheel performance characteristics can be studied. Figures 15 and 16 show the measured and computed distribution of average normal and shear stresses for the level and sloped (4 degree) cases, respectively. Measured slip in both cases was 17 percent. The computed and measured load, torque, and drawbar pull values are shown in Table 1.

5. EXTENSION OF THEORY FOR THE PREDICTION OF TIRE PERFORMANCE

Rigid wheel performance closely approximates that of tires if the stiffness of the tire is great relative to the soil. For less

stiff tires it is necessary to take the effect of tire deformation on soil reaction into account.

Tire deformation affects soil-tire interaction in two ways: it changes the geometry of the soil-tire interface, and it relieves the stresses that would develop in the soil if the interface were undeformable.

A soil-tire model that allows the consideration of all essential factors affecting tire performance is shown in Fig. 17. The tire is assumed to have a constant width both in the undeformed and in the deformed state. The stresses across the tire width are assumed to be uniform so that the soil-tire interaction problem can be treated as two dimensional. Tire deformation is represented by the shape of the tire in the center plane in the direction of travel. Tire shape is assumed to be the same in all parallel planes. The deformation is assumed to consist of two curvilinear segments separated by a linear or flat section. It is assumed that the tire starts to deform an angle α' ahead of the entry angle (α_e), and reaches its original form an angle α'' past the exit angle α_r. In the front curvilinear segment, the radii decrease according to a logarithmic relationship.

The interface stresses between the entry angle, α_e and α_d, as well as those between the exit angle, α_r and α_d, are assumed to be controlled by failure conditions in the soil. Outlines of the respective slip line fields are shown by dashed lines in Fig. 17. The geometry of these failure zones and the associated stresses are computed the same way as for rigid wheels. In the flat portion of the tire the soil pressure equals P_ℓ, a limit pressure characteristic of the tire and inflation pressure.

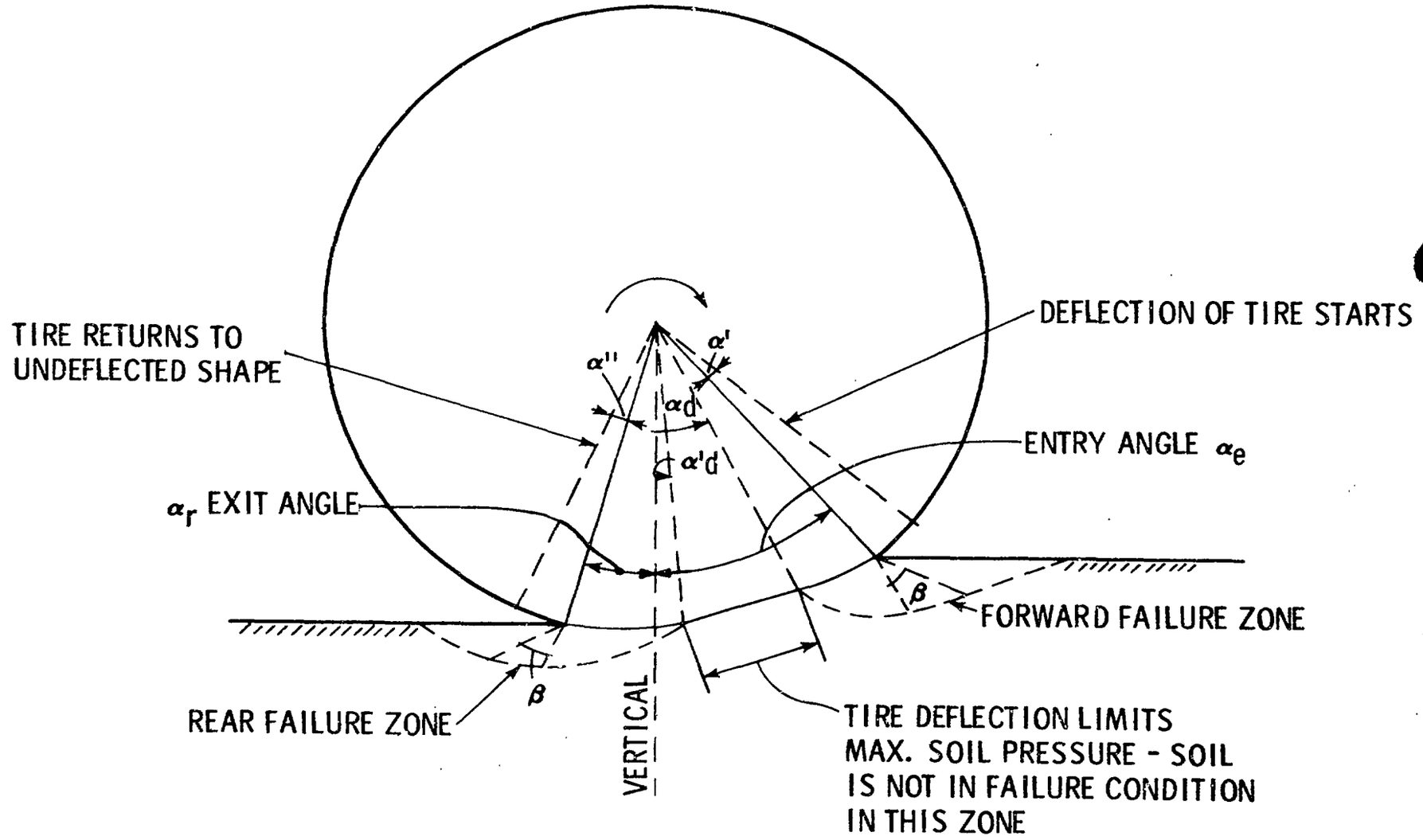

Fig. 17 Soil-Tire Model

Preliminary work with this model indicates that experimental results can be duplicated with the model reasonably well (Ref. 10). We plan to incorporate this model in our computer program so that our method of tractive force prediction would be applicable to both rigid wheels and tires.

6. SUMMARY

The experimental results obtained for a variety of soil conditions indicate that the concept of soil-wheel interaction presented in Section 3 is valid, and interface stresses developing beneath rigid wheels are controlled by soil failure conditions. The numerical integration of the differential equations of plasticity for soils is the basic tool used in determining interface stresses for the boundary conditions imposed by the wheel. Application of these principles to the determination of wheel performance parameters results in a predictive method directly related to soil strength parameters.

In the development of the theory of soil-wheel interaction it was necessary to make certain assumptions as to the development of the interface friction and slip. The interface friction angle, δ, was assumed to be uniform over the perimeter of the wheel. Although in most of the experiments this assumption was found to be approximately correct, in some experiments on clay the interface friction angle was found to increase monotonically from the entry angle toward the rear angle. Although such a behavior was found not to affect the wheel performance parameter prediction excessively, further research could clarify the cause of such behavior and allow appropriate modification of this assumption.

The other area where further experimental information would be most useful is the shear stress-slip relationship. It would be desirable to establish appropriate constants for the various types of soils as a function of strength properties so that such relationships could be used in predictive methods.

ACKNOWLEDGMENT

The major portion of the work reported in this paper was sponsored by the U.S. Army Tank Automotive Command, Warren, Michigan, under Contract No. DAAE 07-72-C-0033.

REFERENCES

1. Karafiath, L., "Plasticity Theory and the Stress Distribution Beneath Wheels," Journal of Terramechanics, Vol. 8, No. 2, 1971.

2. Sokolovskii, V., Statics of Granular Media, Pergamon Press, Oxford, 1965.

3. Nowatzki, E. and Karafiath, L., "General Yield Conditions in a Plasticity Analysis of Soil-Wheel Interaction," paper presented at the Eighth U.S. Regional Off-Road Mobility Symposium, October 1972, Purdue University.

4. Karafiath, L., "On the Effect of Pore Pressures on Soil-Wheel Interaction," Proceedings of the 4th International Conference of the ISTVS, Stockholm, April 1972.

5. Karafiath, L. and Nowatzki, E., The Effect of Speed on Wheel Drag in Soil, Grumman Research Department Memorandum RM-546, July 1972.

6. Sela, A., The Shear to Normal Stress Relationship between a Rigid Wheel and Dry Sand, U.S. ATAC Land Locomotion Laboratory Report, June 1964.

7. Karafiath, L. and Nowatzki, E., "Stability of Slopes Loaded over a Finite Area," Highway Research Board Record No. 323, November 1970.

8. Harr, M., Foundations of Theoretical Soil Mechanics, McGraw-Hill Book Co., 1966.

9. Nowatzki, E. and Karafiath, L., "The Effect of Cone Angle on Penetration Resistance," presented at 51st Annual Meeting of Highway Research Board, Washington; also Grumman Research Department Memorandum RM-532J, January 1972.

10. Karafiath, L., "Soil Tire Model for the Analysis of Off-Road Tire Performance," presented at the 8th U.S. National Off-Road Mobility Symposium (ISTVS), Purdue; also Grumman Research Department Memorandum RM-541, 1972.

11. Janosi, Z. and Hanamoto, B., "The Analytical Determination of Drawbar Pull As a Function of Slip for Tracked Vehicles in Deformable Soils," Proceedings, 1st International Conference on the Mechanics of Soil Vehicle Systems, Torino, 1961.